Connectivity, excitability and activity patterns in neuronal networks

2014 Phys. Biol. 11 036005

(http://iopscience.iop.org/1478-3975/11/3/036005)

IOP Publishing Physical Biology
Phys. Biol. 11 (2014) 036005 (11pp) doi:10.1088/1478-3975/11/3/036005

Connectivity, excitability and activity patterns in neuronal networks

Joost le Feber[1,2], Irina I Stoyanova[1] and Michela Chiappalone[3]

[1] University of Twente, Department of Biomedical Signals and Systems, MIRA Institute for Biomedical Engineering and Technical Medicine, PO Box 217, 7500 AE, Enschede, The Netherlands
[2] University of Twente, Department of Clinical Neurophysiology, PO Box 217, 7500 AE, Enschede, The Netherlands
[3] Istituto Italiano di Tecnologia (IIT), Department of Neuroscience and Brain Technologies (NBT), I-16163 Genova, Italy

E-mail: j.lefeber@utwente.nl

Received 20 December 2013, revised 17 March 2014
Accepted for publication 1 April 2014
Published 15 May 2014

Abstract

Extremely synchronized firing patterns such as those observed in brain diseases like epilepsy may result from excessive network excitability. Although network excitability is closely related to (excitatory) connectivity, a direct measure for network excitability remains unavailable. Several methods currently exist for estimating network connectivity, most of which are related to cross-correlation. An example is the conditional firing probability (CFP) analysis which calculates the pairwise probability ($CFP_{i,j}$) that electrode j records an action potential at time $t=\tau$, given that electrode i recorded a spike at $t=0$. However, electrode i often records multiple spikes within the analysis interval, and CFP values are biased by the on-going dynamic state of the network. Here we show that in a linear approximation this bias may be removed by deconvoluting $CFP_{i,j}$ with the autocorrelation of i (i.e. $CFP_{i,i}$), to obtain the single pulse response ($SPR_{i,j}$)—the average response at electrode j to a single spike at electrode i. Thus, in a linear system SPRs would be independent of the dynamic network state. Nonlinear components of synaptic transmission, such as facilitation and short term depression, will however still affect SPRs. Therefore SPRs provide a clean measure of network excitability. We used carbachol and ghrelin to moderately activate cultured cortical networks to affect their dynamic state. Both neuromodulators transformed the bursting firing patterns of the isolated networks into more dispersed firing. We show that the influence of the dynamic state on SPRs is much smaller than the effect on CFPs, but not zero. The remaining difference reflects the alteration in network excitability. We conclude that SPRs are less contaminated by the dynamic network state and that mild excitation may decrease network excitability, possibly through short term synaptic depression.

Keywords: cultured cortical networks, network bursts, excitability, connectivity, cross-correlation, carbachol, ghrelin

(Some figures may appear in colour only in the online journal)

Introduction

Neuronal excitability at the cellular level has been described as the relation between excitatory and inhibitory forces. In the simplest neuronal setting, this relation translates into the propensity of a neuron to generate an output signal—the action potential (AP)—given an input signal that exceeds a certain threshold (usually an excitatory postsynaptic potential, EPSP). The coupling between neuronal inputs and outputs in the form of EPSP and APs is essential for neurotransmission [2]. The strength of this coupling may vary and is referred to as excitability.

Hyper excitability supposedly underlies diseases like epilepsy [3]. Therefore, most antiepileptic drugs aim to reduce the amount of activity, either by impeding excitation or by enhancing inhibition. Still, 30–40% of epilepsy patients do not respond to these drugs. Despite significant efforts to develop new antiepileptic medications over the past decade, this percentage has remained relatively stable, possibly because the available medication has not addressed all causes of hyper excitability. This suggests that certain forms of epilepsy may have causes other than hyper excitability at the cellular level.

Several studies suggest that hyper excitability may also arise as a network phenomenon, induced by insufficient external input. Network excitability may be defined as the ease with which a network response can be induced by a stimulus. Here, we define network excitability as the mean network response to a spike in one neuron, averaged across all possible presynaptic neurons. When using multi-electrode arrays (MEAs) to measure network activity, the signals from most neurons are not recorded and the electrodes may pick up signals from more than one neuron. Therefore, we adjusted our definition of network excitability to be the array wide mean response to an AP recorded at a certain electrode, averaged across all electrodes.

In hyper excitable networks, a small stimulus (or even no stimulus at all) may induce bursts of activity as seen during epileptic seizures. In fact, several forms of epileptic firing have been associated with low input, like electrical status epilepticus during sleep [4]. During anesthesia, periods of very low afferent input may also occur. Indeed, many anesthetics have been reported to produce seizure patterns in EEG associated with convulsions [5]. In *in vitro* preparations of horizontal hippocampal/limbic cortical slices, deafferentiation increased the sporadic spontaneous epileptiform activity [6]. Moreover, organotypic hippocampal slice cultures usually develop spontaneous ictal-like activity patterns in response to slicing induced deafferentiation [7]. These observations all suggest that sensory input might have a suppressive effect on cortical population bursts [8].

Acute electrical stimulation [1, 9] or pharmacological treatment of *in vitro* preparations of neuronal tissue [10, 11] have been shown to transform neural bursting patterns into more dispersed one firing. Both manipulations, however, were only effective within a narrow window of moderate parameter settings, and could also induce adverse effects. For example, electrical stimulation at a very low frequency (<0.2 Hz) usually triggered population bursts rather than suppress them. Stimulus induced population bursts probably occur because the network is already in a hyper excitable state and stimulation at such frequencies are insufficient to continuously reduce the network excitability. In cultured cortical networks, pharmacological desynchronization only succeeds with mild excitatory agents—such as acetylcholine (ACh), orexin, serotonin, ghrelin etc. Straightforward excitants like glutamate or aspartate do not suppress epileptiform bursting, but instead enhance bursting at specific concentrations [12]. The outcome of either manipulation depends on the delicate balance between two factors: (strong) stimuli that may induce excessive responses or even trigger seizures in networks that are already hyper excitable may also reduce network excitability which leads to smaller stimulus responses and less population bursts. Thus, 'restoring' moderate input strongly decreases, or even abolishes excessive synchronization. It has been hypothesized that insufficient activity within neural networks leads to a very low average level of synaptic/neuronal depression [13, 14] or homeostatic up regulation of excitability [15–17], thus yielding hyper excitable networks.

Although hyper excitability is a crucial factor in diseases such as epilepsy or Parkinson's disease [26] and has been related to disorders like phantom pain [27], tinnitus [28] and amnestic mild cognitive impairment [29], there is currently no tool to quantify network excitability. Obviously, network excitability is closely related to (excitatory) connectivity and several methods currently exist for estimating network connectivity. We developed an analysis of network connectivity based on conditional firing probabilities (CFPs). $CFP_{i,j}[\tau]$ is the probability that electrode j will record an AP at time $t=\tau$, given that electrode i recorded a spike at $t=0$. We refer to electrodes rather than neurons in our definition because we do not discriminate between the activity from individual neurons that may be recorded by the same electrode. Because electrode i often records multiple spikes within the analysis interval (typically 500 ms) and the response to the first spike cannot be discriminated from those from subsequent spikes, CFP values are biased by the dynamic state of the network (e.g. bursting patterns vs. dispersed firing). In particular, network bursts may cause a bias that we will refer to as multiple input spike bias. This bias also exists in other cross-correlation based measures. We will show that this bias may be removed in a linear approximation by deconvolution of the autocorrelation from the CFP. This procedure provides the average response at electrode j to a single spike at electrode i (single pulse response, $SPR_{i,j}$). Thus, in a linear system, SPRs are independent of the dynamic network state. However, nonlinear components such as facilitation and short term depression will still be reflected in SPRs. Since they are not biased by multiple input spikes within the analysis interval, SPRs will provide a cleaner measure of network excitability than traditional cross-correlation based methods.

We will evaluate SPRs in cultured networks of cortical neurons on MEAs. In the absence of external input, such networks usually develop bursting firing patterns [18]. It is hypothesized that these bursts result from excessive network excitability. We will apply cholinergic stimulation to activate these cortical networks. ACh is a neuromodulator with a net excitatory effect on cortical networks. Since it is not synthesized in the cortex, ACh does not directly affect the existing excitatory (glutamatergic) connections. It does however affect the dynamic network state. In addition, we will apply ghrelin, another neuromodulator that induces moderate neural activation, to the cultures. We will show that cholinergic or ghrelinergic activation changes the activity patterns from predominant synchronous bursting to more dispersed firing. This change in network dynamics may affect CFPs in two ways: (1) the multiple input spike bias will change, and (2) network excitability may change. The multiple input spike

bias will cause an overestimation of the CFP values in a bursting dynamic state. SPRs are only affected by this second factor. Excitability changes may mask the effect of multiple input spike bias or alternatively enhance it, depending on the direction of change. Assuming that bursting patterns result from high network excitability, multiple input spike bias most likely enhances the increase of CFPs due to higher excitability in a bursting dynamic state. Therefore, we expect that SPRs are less affected than CFPs by dynamic state changes. We will validate this hypothesis using carbachol (CCh) or ghrelin and we will confirm that periods of more pronounced bursting indeed coincide with higher network excitability.

Methods

Cell cultures

We obtained cortical cells from newborn Wistar rats on post natal day 1. After trypsin treatment, cells were dissociated by trituration. About 400 000 dissociated neurons (400 μl suspension) were plated on a multi electrode array (MEA; Multi Channel Systems, Reutlingen, Germany), precoated with poly ethylene imine. This procedure resulted in an initial cell density of approximately 5000 cells mm^{-2}, in agreement with the counted estimates in the first few days after plating. With aging, cell densities gradually decreased to ~2500 cells mm^{-2}. We used MEAs containing 60 titanium nitride electrodes with a 30 μm diameter and 200 μm pitch.

Neurons were cultured in a circular chamber with inner diameter $d = 20$ mm that was glued on top of the MEA. The culture chamber was filled with ~700 μL R12 medium [19] MEAs were stored in an incubator, under standard conditions of 37 °C, 100% humidity, and 5% CO_2 in air. For recordings, we firmly sealed the culture chambers with watertight but CO_2 permeable foil (MCS; ALA scientific), and placed the cultures in a measurement setup outside the incubator. During recordings, we maintained the CO_2 level of the environment around 5% and we maintained humidity. For details about the recording setup, see [20]. Recordings began after an accommodation period of at least 20 min. After the measurements, the cultures were returned to the incubator. We used seven CCh and nine ghrelin treated neuronal cultures obtained from different rats. All CCh experiments were performed at least 20 days after plating of the dissociated cells ghrelin experiments were done at 10 ± 0.6 days after plating.

Activity recording and analysis

Data was recorded from all electrodes at a sample rate of 16 kHz, using a custom program that estimated the noise levels for each electrode in real time. Potential spikes were stored whenever the signal exceeded a predefined threshold of 5.5 times the estimated noise level. For each spike, the program stored the time stamp, the recording electrode on which it was detected, and 6 ms of the spike waveform, from 2 ms before the threshold crossing to 4 ms thereafter.

We applied a method introduced by Wagenaar *et al* [1] to estimate the burstiness of a culture on a minute-order time scale. In short, 5 min recordings were divided into 300 1 s long time bins and then number of spikes across all electrodes in each bin was tallied. We then computed the fraction of spikes accounted for by the 45 bins (15% of all bins) containing the largest spike counts ($f15$). Should most of the spikes occur in bursts, $f15$ will be close to 1; tonic firing should lead to a $f15 \approx 0.15$. We then defined a burstiness index (BI) such that $BI = (f15 - 0.15)/0.85$, so that BI is normalized between 0 (no bursts) and 1 (burst dominated).

We also analyzed firing and bursting patterns using the algorithms introduced by Bologna *et al* [21]. In short, bursts were detected whenever at least five spikes were recorded, with a maximum inter spike interval of 100 ms. For each 300 s interval, the mean firing rate (MFR), burst intensity, burst duration and dispersed fraction (DF; the fraction of spikes detected outside bursts, see [22]) were determined.

Connectivity analysis

Several techniques have been developed to estimate network connectivity based on the timing of spiking activity patterns. Very often, these methods are based on or related to cross-correlation. In our lab, we developed a technique based on CFPs ($CFP_{i,j}[\tau]$) to estimate functional connectivity [23]. This technique provides intuitive measures of the strengths and latencies of functional connections and has been shown to, at least to a certain extent, describe synaptic connections in cultured cortical networks [24].

CFP analysis evaluates all spiking activity during the 500 ms after any recorded AP by calculating the probability that electrode j recorded an AP at $t = \tau$ given that electrode i did so at $t = 0$. To calculate the CFP, we first represent the spike time series as a binary point process $X_i[t]$ in which ones and zeroes represent whether a spike was detected at electrode i at time t. Thus, the number of APs at the initiating electrode i followed by a spike at the responding electrode j with a delay of τ ($N_{\text{follow}i,j}[\tau]$) is calculated as follows:

$$N_{\text{follow}_{i,j}}[\tau] = \sum_t X_i[t] \cdot X_j[t + \tau]. \quad (1)$$

Equation (1) holds because it is applied to binary arrays X_i and X_j, with $X_i,[n] \in \{0, 1\}$ for all n. CFP[τ] can be calculated by dividing $N_{\text{follow}}[\tau]$ by the total number of APs at electrode i (N_i):

$$\text{CFP}_{i,j}[\tau] = \frac{N_{\text{follow}}}{N_i} = \frac{\sum_t X_i[t] \cdot X_j[t + \tau]}{\sum_t X_i[t]} \; \forall \; 0 < \tau < 500\,\text{ms}. \quad (2)$$

This analysis yields a probability curve, to which a four-parameter standard function (equation (3)) is fitted to obtain measures for the strength ($M_{i,j}$) and latency ($T_{i,j}$). The additional variables $w_{i,j}$ and $\text{offset}_{i,j}$ are necessary for curve fitting, but are not used in further analyses. For detailed explanations,

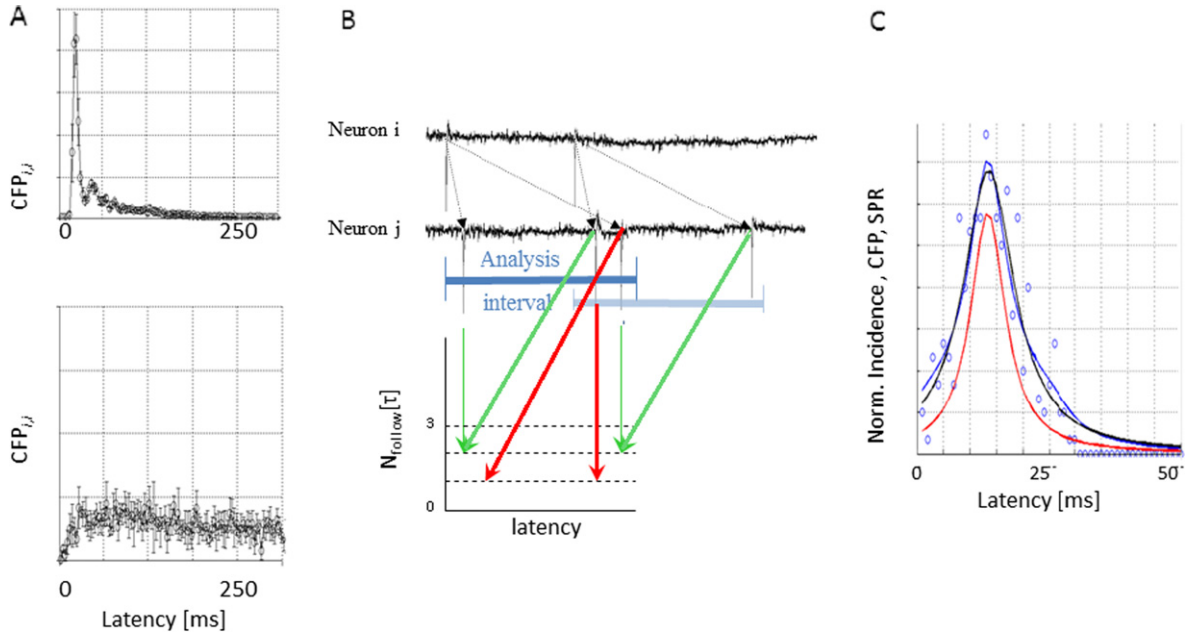

Figure 1. CFP$_{i,i}[\tau]$ (autocorrelation) and its effect on the estimated functional connectivity. (A) Two examples of CFP$_{i,i}[\tau]$, the probability that electrode i records an action potential at time $t=\tau$, given that it also recorded one at $t=0$. This conditional probability is proportional to the autocorrelation. Although some flat autocorrelations (bottom window) can be found (~20%), most electrodes are associated with an autocorrelation as shown in the top window (~80%). This indicates that electrodes are likely to pick up more than one action potential in the analysis interval. (B) A hypothetical situation in which each spike from the presynaptic neuron i induces a fast and a slow response in the post synaptic neuron j, as indicated by the gray lines. To estimate CFP$_{i,j}[\tau]$, all spikes of neuron j are counted in fixed analysis time intervals (indicated by blue horizontal bars) after each presynaptic spike. Because these time intervals partially overlap, in the calculation of N_{follow} (see equation (1)), responses are not only counted in the analysis interval directly after the corresponding presynaptic spike (green arrows), but also in the analysis interval after the other presynaptic spike (red arrows). Multiple spikes from neuron i during the analysis interval thus contaminate the estimation of the average response of neuron j to a spike from neuron i (multiple input spike bias). (C) To obtain an estimate for the CFP's, the incidence of postsynaptic action potentials is counted during a 50 ms time interval after the presynaptic spike (○). A standard equation (equation (3)) was fitted to the data (black line) to obtain the CFPs. SPRs were calculated by convolving the standard function with the autocorrelation of the presynaptic neuron during this fitting process (red line). The blue line indicates the convolution of the SPR with the autocorrelation, which approximates the CFP.

see [23].

$$\text{CFP}_{i,j}^{\text{fit}} = \frac{M_{i,j}}{1 + \left(\dfrac{\tau - T_{i,j}}{w_{i,j}}\right)^2} + \text{offset}_{i,j}. \tag{3}$$

The measure in equation (3) does not reveal responses to single input spike because the initiating electrode i usually records more than one spike during the analysis interval. Thus, a late response in electrode j may be attributed to a later spike recorded at electrode i and a fast response in electrode j may be attributed to a preceding spike at electrode i. This introduces a bias, which we refer to as the multiple input spike bias (see Introduction). For an example see figure 1.

On average, this repeated firing may be captured by CFP$_{i,i}[\tau]$ which is proportional to the auto correlation function of the initiating electrode i. To avoid confusion between CFP$_{i,j}[\tau]$ and CFP$_{i,i}[\tau]$ we will refer to the latter as the auto-correlation. For linear time invariant systems, the output of a system in the frequency domain $Y(\omega)$ is calculated by taking the product of the input $X(\omega)$ and the transfer function $H(\omega)$ (equation (4)). This is equivalent in the time domain to taking the convolution of the input $x(t)$ with the impulse response $h(t)$ (equation (5)).

$$Y(\omega) = X(\omega) \cdot H(\omega), \tag{4}$$

$$y(t) = x(t) \otimes h(t) = \int_{-\infty}^{\infty} x(t-\tau) \cdot h(\tau) \mathrm{d}\tau. \tag{5}$$

Here, $\otimes$ denotes the convolution operator. On average, the input from electrode i may be described by the autocorrelation (CFP$_{i,i}[\tau]$), the probability that it records an AP at $t=\tau$, given that it previously recorded a spike at $t=0$. This implies that, in a linear approach, we may deconvolve the input (auto-correlation) from the output (CFP) to obtain an 'impulse response'. This relationship can be deduced from equation (5) as follows:

$$y(t+\tau) = x(t+\tau) \otimes h(t), \tag{6}$$

$$\sum_{t=0}^{n} x(t) \cdot y(t+\tau) = \sum_{t=0}^{n} x(t) \cdot x(t+\tau) \otimes h(t), \tag{7}$$

$$\frac{\sum_{t=0}^{n} x(t) \cdot y(t+\tau)}{\sum_{t=0}^{n} x(t)} = \frac{\sum_{t=0}^{n} x(t) \cdot x(t+\tau)}{\sum_{t=0}^{n} x(t)} \otimes h(t), \tag{8}$$

$$\text{CFP}_{i,j}[\tau] = \text{CFP}_{i,j}[\tau] \otimes h(t). \tag{9}$$

However, because neuronal networks are nonlinear systems, we will use the term 'SPR' instead of impulse response, as shown in equation (10).

$$\mathrm{CFP}_{i,j}[\tau] = \mathrm{CFP}_{i,j}[\tau] \otimes \mathrm{SRP}(t). \quad (10)$$

Since deconvolution is a rather unstable process, we avoided it by applying the following procedure. Instead of fitting the standard function of equation (3) directly to the data (which would yield CFP parameters), we convolved the standard function with the autocorrelation during each iteration of the fitting procedure. In this way, we obtained values for the SPR parameters that would yield the CFP curve when convolved with the autocorrelation (equation (10)).

To observe the development of the SPRs, long term recordings were subdivided into data blocks of 2^{15} detected events (see [23]). For all electrode pairs (*i,j*), we calculated the $\mathrm{SPR}_{i,j}[\tau]$ for each data block.

First, we investigated to what extent CFPs were biased by bursting activity patterns. Assuming that multiple spike induced bias may be neglected during periods of dispersed firing (i.e. if autocorrelation curves are flat, convolution with the autocorrelation reduces to rescaling of the CFP curve), the SPRs will be rescaled versions of the CFPs. We noticed that, during the phase of drug (i.e. CCh) application, activity patterns showed the least synchronized firing, and consequently, there was minimum multiple input spike bias (cf results, figures 2 and 3). For this reason, all CFPs and SPRs were normalized to their mean value during CCh treatment in order to observe the extent to which the CFPs exceed the SPRs before and after the CCh phase (i.e. during periods of intense bursting patterns). This measure is indicative of the magnitude of the multiple input spike bias in the CFPs and it provides a good metric for evaluating the different information provided by CFP versus SPR (see results, figure 4).

Then we a statistically assessed the effects of pharmacological manipulations. In general both CFPs and SPRs between various electrode pairs have a wide range of strengths and may differ by a factor of 1000 or more. To determine the effect of changing dynamic conditions on connectivity strength, we treated the cultures with CCh/ghrelin as described below. Application of these substances strongly reduced bursting and transformed the activity patterns to mainly dispersed firing. Because we were interested in the average rather than the absolute value of the effect of changing dynamic conditions on the connectivity strength, provided by our SPR, the strengths of all functional connections were normalized to their mean value during baseline, before averaging across all electrode pairs (see results, figures 5 and 6).

Pharmacological manipulation

For all cultures, we first estimated the functional connectivity in the baseline phase for about 2 h, using SPRs as explained above. We then replaced 300 μL of the medium by 300 μL of CCh (40 μM, Sigma, St. Louis, MO, USA), a selective cholinergic agonist leading to a final CCh concentration of 20 μM. Next, we repeated the analysis to monitor changes in the SPRs during the CCh phase, lasting 18–26 h. Finally, we completely refreshed the medium twice to wash out the CCh and repeated the analysis during this washout phase, for 3–46 h. To assess the stability of functional connectivity within each of the three phases, we divided the control, CCh and washout recordings of all experiments into data blocks of 2^{15} spiking events each, yielding on average ~100 blocks per phase.

In addition, we acutely applied ghrelin (2 μM, Abcam, Cambridge, UK), another neurotransmitter that has been shown to have a moderate excitatory effect on cortical neurons [25]. We investigated the effect on SPRs, and burstiness, MFR, burst duration, burst intensity and DF (see under *Activity recording and analysis*). These additional experiments aimed to reproduce the acute change in firing dynamics from bursting to more dispersed firing, and to show that this change is not specific to CCh. The baseline and ghrelin phase of the experiments lasted one hour each. We did not study the long term effects of ghrelin or the effects of washout.

All results are shown as the mean ± the standard error of the mean, unless indicated otherwise.

Results

We investigated the shape of the autocorrelation curves for all electrodes under control conditions. The autocorrelation indicates the probability of recording a second (or further) AP after a short delay. In approximately 20% of all active electrodes, the $\mathrm{CFP}_{i,i}[\tau]$ curve was flat after an initial refractory period. In 80% of all electrodes, we found curves that clearly showed a peak at certain latencies and harmonics. For example, in figure 1(A), the peak in the autocorrelation occurs at $t = 18$ and 36 ms. Such peaks in the autocorrelation mean that most electrodes are likely to record more than one spikes in the CFP analysis interval of 500 ms. Thus, when deriving correlograms between two recording electrodes *i* and *j*, subsequent spikes detected by electrode *j* may be interpreted as a response to different spikes recorded at electrode *i*, as illustrated in figure 1. Thus, CFP curves are usually biased by multiple correlated spikes from presynaptic neuron(s) at electrode *i*. Figure 1(C) shows an example of the spike counts at electrode *j* at latencies of 0–50 ms, the fitted standard function (equation (3)) to obtain the CFP curve, the estimated SPR, and the convolution of the SPR with the autocorrelation.

We pharmacologically manipulated the dynamical state of the network to evaluate its effects on the CFPs and SPRs. We added CCh to the bath during seven experiments and ghrelin during nine. In general, we observed that bursting activity patterns were transformed into more dispersed firing when either one of these modulatory agents was applied. Figure 2 shows a typical example of the response, characterized by an overall increased firing rate and more dispersed firing after the administration of the agent.

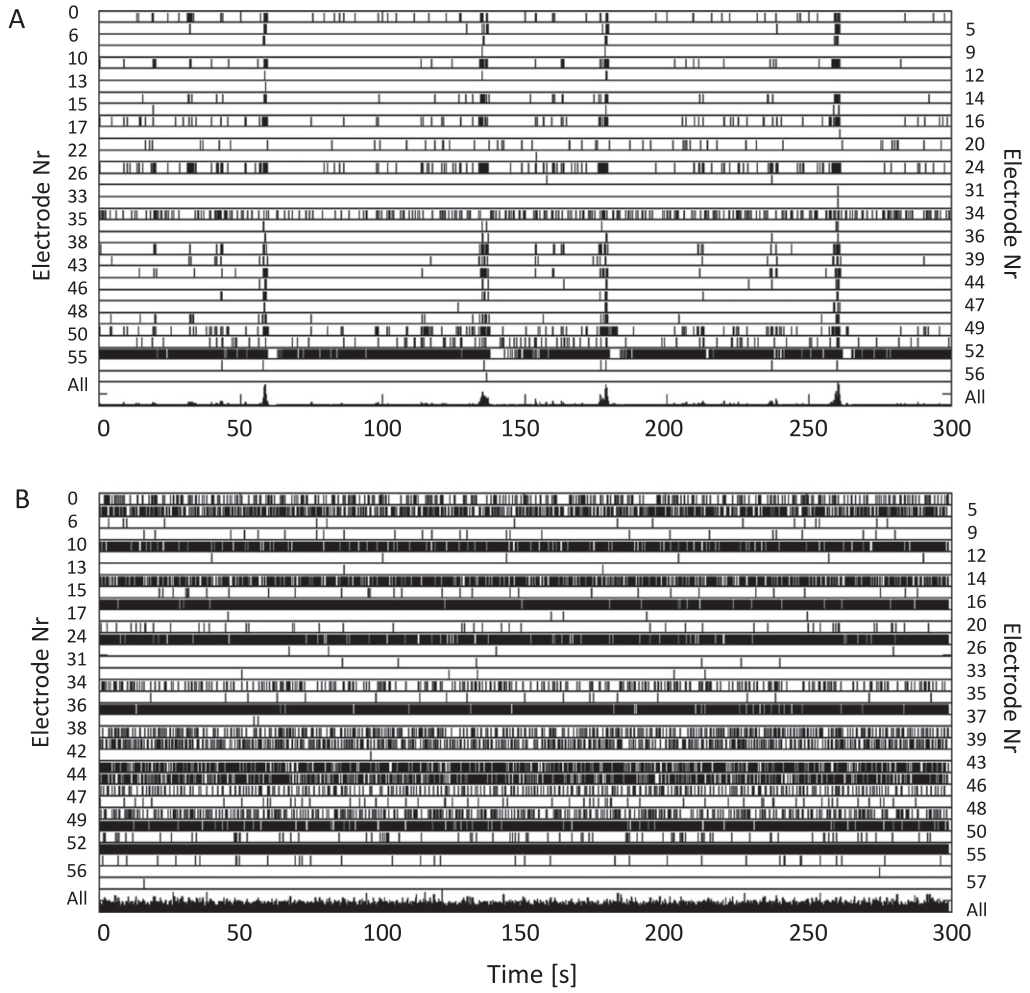

Figure 2. Example of the acute effect of moderate excitation on recorded firing patterns in a 10 day old cortical culture. We recorded the activity before (A) and after moderate pharmacological excitation as induced by ghrelin (B). In both panels, the upper horizontal traces show the activity recorded at the indicated electrode number while the bottom trace indicates the summed activity of all electrodes in 1 s bins. Each tick represents an action potential. Typically, baseline firing patterns contained periods of seemingly uncorrelated spiking as well as synchronized network bursts. Carbachol induced a similar transformation of the activity pattern into more dispersed firing.

CCh experiments

To quantify the different dynamic network states, we calculated the network wide MFR, burst intensity (i.e. the frequency of spikes within a burst), burst duration and DF, the fraction of spikes outside the bursts (see methods). During baseline, the MFR was 1.3 ± 1.3 spikes s^{-1}/electrode. Upon CCh application, the MFR increased by $90 \pm 9\%$. The average burst intensity dropped to $55 \pm 2\%$, while the DF increased by $31 \pm 2\%$. Mean burst duration increased by $113 \pm 7\%$. After CCh washout, none of these measures showed any obvious trend away from the pre-CCh values (figure 3).

Next, we divided all CCh experiments into data blocks of 2^{15} spikes, which yielded 19 ± 14 (mean $\pm$ SD) data blocks in the baseline phase, 201 ± 151 in the carbachol phase, and 95 ± 138 after carbachol washout. To directly compare the CFPs and SPRs under various dynamic conditions, we normalized the CFPs and SPRs to their mean values during the agent's phase. Figure 4 shows normalized CFP and SPR values before, during and after CCh washout. On average, CFPs were larger than SPRs in the phases before CCh application ($40 \pm 19\%$ larger) and after washout ($50 \pm 10\%$ larger). A two-tailed paired *t*-test showed that CFPs and SPRs differed significantly ($p < 0.01$), even though this test included the values during CCh, which naturally did not differ ($p > 0.75$) due to the applied normalization.

We investigated whether changes in the SPR values were correlated to the burstiness of our cultures (see figure 5). We found that in the control phase, SPRs were fairly constant, with an average coefficient of variation (CV; standard deviation as a percentage of the mean value) of 33 ± 13 (SD)%. During CCh treatment, the SPRs dropped to 37 ± 5 (SD)% of their baseline value and the relative CV increased slightly to 41 ± 14 (SD)%. After CCh washout, the normalized SPRs increased with respect to the baseline, showing a significant overshoot (17 ± 8 (SD)%), while the CV dropped again to 36 ± 12 (SD)%. The BI dropped from 0.53 ± 0.04 (SD) during baseline to 0.23 ± 0.04 (SD). After washout, BI returned towards baseline. The tendency to remain below baseline was not significant (Wilcoxon signed rank: $p > 0.06$). Normalized SPRs also increased after washout, but they showed significant overshoot, i.e. after washout (see figure 5).

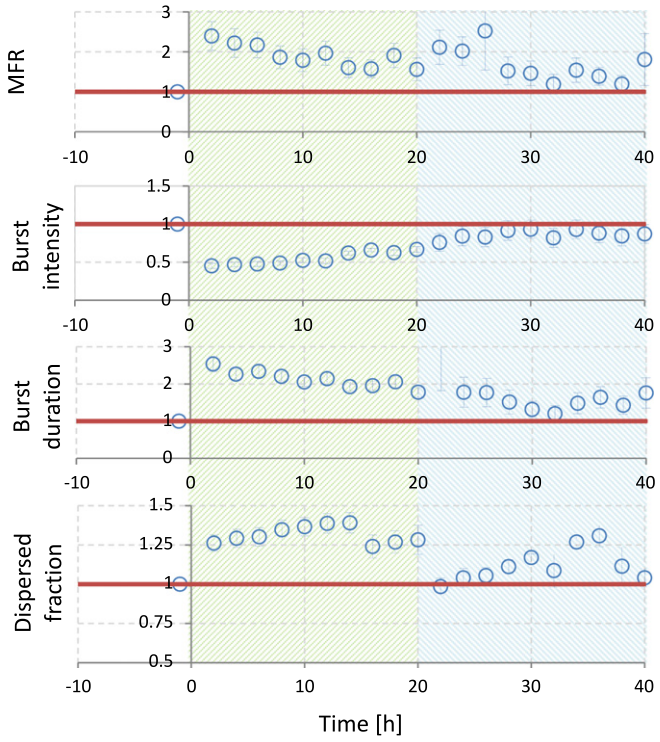

Figure 3. Analysis of burst patterns before ($t<0$, white background), during ($0<t<20$ h, green) and after carbachol application ($t>20$ h, blue). Data was collected from six experiments. The mean firing rate (MFR) was calculated in 2 h bins. Burst intensity was the mean firing rate during bursts. Burst duration was the time between the onset and cessation of bursts. The dispersed fraction indicates the fraction of all spikes that were fired outside the identified bursts periods. All values were normalized to their baseline values. Error bars indicate the standard error of the mean, and refer to the differences between experiments.

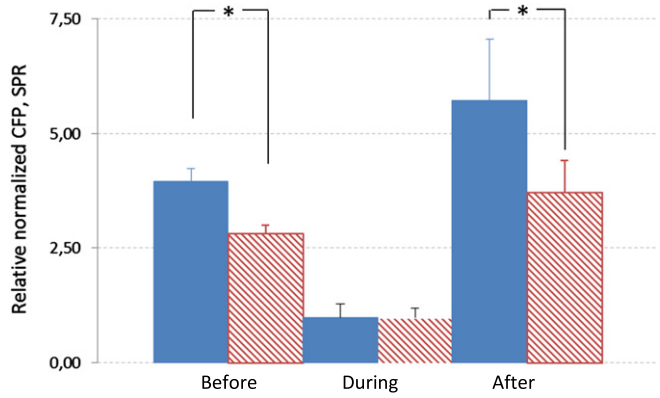

Figure 4. Differences in the mean normalized conditional firing probability (CFP) and single pulse response (SPR), coinciding with changing dynamic network states. In seven cultures, the strength of all persisting connections was normalized to their mean value during carbachol treatment. Average CFPs (solid bars) and SPRs (hatched) are shown before (hours 0–2 of the experiments), during (hours 2–21) and after carbachol application (hours 22–28). Mean values ± SD are shown. * indicates significant differences (two-tailed paired t-test: $p<0.01$).

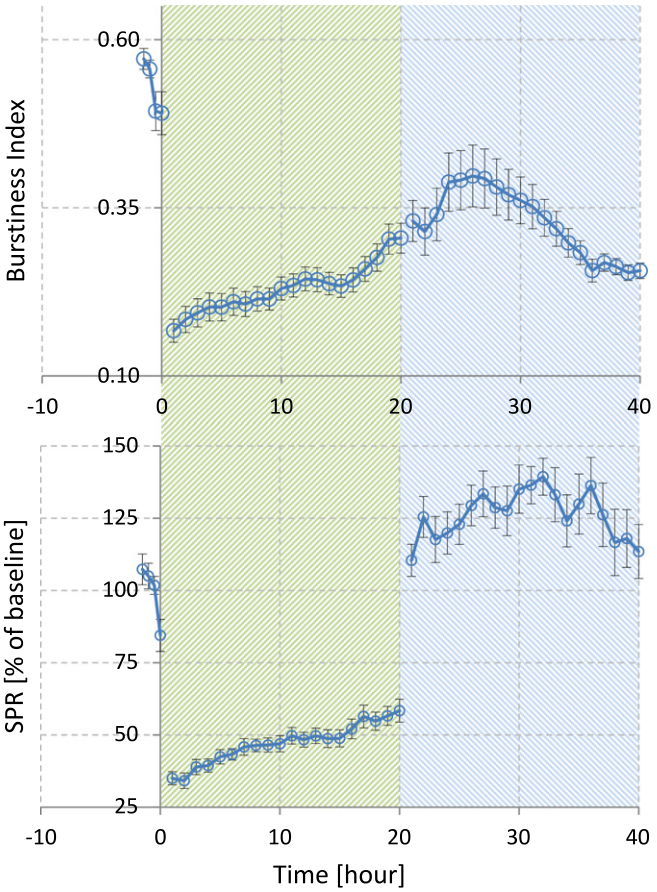

Figure 5. Effect of carbachol on single pulse responses (SPRs) and burstiness index. After two hours of baseline recording ($t<0$, white background), seven cultures were exposed to 20 μM carbachol for at least 20 h ($0<t<20$ h, green background). The culture medium was then refreshed twice to wash out the carbachol and another twenty hours of data was recorded ($t>20$ h, blue background). The burstiness index was calculated as defined in [1].

Ghrelin experiments

In nine cultures, we applied another neuromodulator, ghrelin, to compare the reduced burstiness and SPRs observed during CCh treatment. Again we observed a ~50% decrease in the BI (figure 6). In three experiments, we recorded sufficient APs to calculate the SPRs, which decreased by ~30% on average. Four of the nine experiments had enough bursts to calculate the other parameters (i.e. MFR, burst intensity, burst duration and DF). The results were comparable to those during CCh application: the firing rate and dispersed fraction increased by 150% and 60% respectively, while burst intensities and durations were not noticeably affected (data not shown).

Discussion

Network excitability is obviously closely related to excitatory network connectivity, and there exist several measures to quantify connectivity. However, currently available cross-correlation based methods yield connectivity measures that

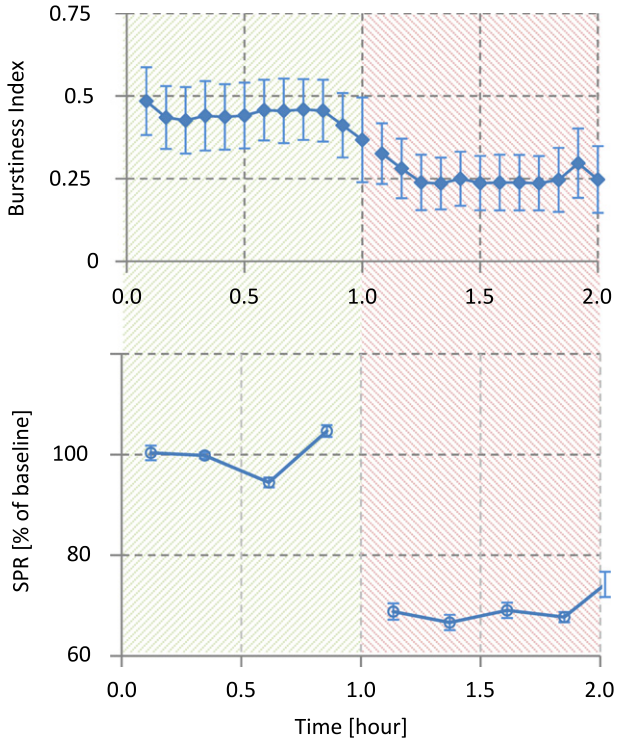

Figure 6. The effect of ghrelin on burstiness and single pulse responses. One hour of data was recorded prior to ghrelin administration (green background) and the burstiness index (BI) was calculated for nine experiments and averaged (top panel). Only three experiments contained enough action potentials to calculate the SPRs (bottom) and evaluate the effect of ghrelin (red background) on excitability. The BIs were calculated for each 5 min bin while the SPRs were calculated from periods of variable length that contained 2^{15} spikes. Values across the three experiments were pooled using 15 min bins.

are biased by the dynamic state of the network (multiple input spike bias). In a linear approximation, this multiple input spike bias may be removed by deconvolution of the auto-correlation. This mathematical manipulation allowed us to obtain the SPR which is independent of the dynamic network state. However, nonlinear components of synaptic transmission, such as facilitation and short term depression, still affected SPRs. Indeed, dynamic state (bursting) induced changes affected SPRs significantly less than CFPs, but its influence on SPRs was not entirely zero. Unbiased by multiple input spikes, SPRs provide a cleaner measure of network excitability than traditional cross-correlation based methods. Theoretically, the remaining effect of dynamic network state on SPRs better reflects differences in network excitability than the shifts in CFP values. We compared SPRs to burst characteristics to validate that network bursting is more intense when network excitability is (too) high.

CFPs as well as SPRs were determined for all pairs of electrodes, which cannot always be directly translated into pairs of neurons. Some studies applied spike sorting algorithms, usually based on differences in the shapes of APs. At some electrodes the shape of recorded APs was highly reproducible, but often wave shapes varied, depending on background activity in the network, possibly due to superimposed local field potentials. Occasionally we recorded APs of decaying amplitude during a single burst. These factors make it troublesome to use spike sorting as a tool to discriminate between different neurons. For the analyses in this paper, it was not necessary to discriminate between spikes from different neurons. Rather, we used the small groups of neurons which were in good contact with the electrodes as the unit to determine functional connectivity, as also reported in other papers [1, 30, 31].

To avoid inverse convolution, we convolved the standard function in equation (3) with the autocorrelation during each iteration step in the fitting procedure. This approach assumes that the SPRs share the same general shape of CFP's, as depicted in figure 1. This assumption was supported by the observation that the electrodes that had a flat autocorrelation (~20%) under control conditions, showed probability curves with the same shape as the electrodes with nonflat autocorrelations (80%) [23]. Besides the initiating electrode *i*, the responding electrode *j* may also record more than one spike in the analysis interval. Obviously, the firing rate of *j* also depends on the dynamic network state. However, this does not introduce additional bias because only those spikes recorded at electrode *j* that are time locked to spikes recorded at electrode *i* contribute to the strength of a functional connection ($M_{i,j}$ in equation (3)); other spikes at electrode *j* only affect the value of the offset parameter.

It is well known, that short term plasticity affects synaptic strengths in a frequency dependent manner, and that individual input spikes therefore do not induce a consistent SPR. However, under stationary dynamic conditions, the SPR stabilizes when averaged over relatively large time windows. We used data blocks of 2^{15} spikes, which lasted ~20 min on average. Such periods are large enough to contain numerous network bursts, as well as multiple phases of seemingly uncorrelated firing. This resulted in reliable, reproducible SPRs over consecutive windows, as indicated by the low intra-individual CV during the two hour control phase (~33%, figure 5). During and after CCh application, the CVs were slightly higher, possibly reflecting an initial adaptation after a sudden change in the dynamics, or due to the longer duration of these recording periods (~24 versus ~2 h). However, the CVs were still relatively low, indicating that the effects of short term plasticity mechanisms on connectivity were fairly constant within each phase.

Cholinergic stimulation changed firing patterns from bursting into more dispersed activity (see figure 2). This was partially demonstrated in previous studies [11–32], possibly due to reduced signal propagation. It has been shown that ACh suppresses the spread of excitation in visual cortex, and that the site of the cholinergic action is presynaptic [33]. These observations are in agreement with the hypothesis that short term depression decreases network excitability [34]. Kimura *et al* [33] concluded that the predominant role of Ach is to change the overall state of cortical circuits, or specifically, to shift the dynamics of cortical circuits from being predominantly influenced by intrinsic activity to being influenced by thalamocortical input. This conclusion agrees with our finding that predominant intrinsic activity patterns

(network bursts) largely disappeared upon cholinergic activation. The CCh phase showed a slowly fading effect on most parameters, as shown in figure 3, possibly due to adaptation of the neurons or degradation or depletion of the CCh. Our wash out procedure not only removed the remaining CCh from the medium, but also other neuronal substances that are important for network functioning, such as brain derived neurotropic factor. The latter may also affect the activity level and pattern, obscuring the interpretation of post-CCh data. Therefore, we could not draw stronger conclusions than the observation that, none of these measures showed an obvious difference from pre-CCh values after washout. Because of the difficult interpretation of the data recorded after washout, we did not include this phase in the ghrelin experiments that were done after the experiments with CCh.

We used CCh, rather than ACh because CCh is resistant to hydrolyzing enzymes and could be present in the medium during the 24 h CCh phase, and the effects on the cortical networks are comparable at medium concentrations. Application of a medium concentration of CCh (10–50 μM) causes a switch from synchronized bursting to more asynchronous single spike mode of spontaneous firing pattern through muscarinic receptor activation, while ACh application at concentration of 10–50 μM inhibits synchronized bursting [35]. Although this general effect of cholinergic activation is well known, the underlying mechanism of action is still under debate. In an intracellular study, Klink and Alonso demonstrated several sub threshold changes during CCh modulation, in addition to changes in the frequency of intrinsic firing and AP shape [36]. Differences in sub threshold dynamics disappear under ttx blockade, indicating that sodium influx is involved, but its exact role remains unclear. Their results point towards increased intrinsic bursting in some cells rather than more dispersed firing, suggesting that the mechanism behind the desynchronizing effect of cholinergic activation is not at the cellular level. Here we hypothesize that desynchronization may be a network phenomenon. Mild excitation of networks with little or no ongoing activity may induce a higher degree of short term depression in recurrent excitatory synapses and thus reduce network excitability. This hypothesis is supported by the finding that ghrelin also desynchronized network activity, very similar to CCh. Furthermore, Wagenaar *et al* [1] showed that the firing patterns of isolated cortical networks also transformed to more dispersed firing when the firing rate was increased by closed loop electrical stimulation. In that study, the BI decreased almost linearly with the array wide firing rate. However, complete transformation required a much larger increase in firing rate than the CCh induced increase in our study. Seemingly adverse results obtained by Leondopulos *et al* showed that chronic electrical stimulation induced shorter and more intense bursts [37]. However, in their experiments, burstiness was evaluated after cessation of the electrical stimuli.

Application of either neuromodulators increased the network wide activity, while reducing the incidence of synchronized firing and strength of the functional connections. Our results do not provide direct evidence to discriminate cause and effect. Less synchronized firing might result from weaker functional connections or, vice versa, the strength of functional connectivity may appear to decrease when fewer network bursts occur and therefore fewer spikes will fall within the 500 ms analysis interval. During bursts, however, synaptic strengths usually decrease due to short term synaptic depression; bursts in isolated networks are terminated by synaptic depression, refractoriness and cellular adaptation, rather than by activation of the inhibitory system [14]. In cats, evoked excitatory postsynaptic potentials (EPSPs) in the neocortex increased around seizure onset and returned to baseline between seizures [13]. It has been shown that functional connections reflect to a certain extent synaptic properties [24]. Therefore, it is probable that functional connections weaken during each burst. During periods of dispersed firing, most neurons fire at a low frequency, with inter spike intervals that exceed the decay time of short term synaptic depression. Nevertheless, most synapses, as well as most functional connections, will be stronger than during dispersed firing than during bursts. Thus, periods without extensive bursting should yield relatively strong functional connections, and it seems unlikely that reduced bursting (as seen during CCh or ghrelin treatment) would lead to weaker functional connectivity. Therefore, the most probable explanation is that the average connectivity strength decreased and consequently, synchronized firing decreased as well. This view is supported by the finding that muscarinic receptor activation reduced the size of EPSPs in diverse cortical synapses [38]. Likewise, computer modeling showed that the effects of ACh could be reproduced by decreased synaptic conductances between cortical pyramidal cells [39]. A critical factor is the average firing frequency, which should be high enough to induce short term synaptic depression. The baseline firing frequency of ~1.3 spikes s^{-1}/electrode yields average inter spike intervals of ~800 ms, which is on the order of the decay time of short term synaptic depression [40]. CCh application almost doubled the MFR, thus reducing the mean inter spike interval to values that frequently induce short term depression.

There are other mechanisms, besides those mentioned above, that affect network excitability. Homeostatic mechanisms have been described that generate more sensitive excitatory synapses and less or weaker inhibitory synapses (15–17). A prolonged period of insufficient activity will lead to strengthened excitatory connectivity which may result in a hyper excitable network that generates bursting firing patterns when activated. However, if homeostatic synaptic scaling were the dominant mechanism, excitability should have been lower after 24 h of cholinergic stimulation, which contradicts our results. Furthermore, the changes in the SPR and BI appeared almost instantaneously, which does not correspond to the time constant of synaptic scaling. Therefore, it seems unlikely that excitability changes result from synaptic scaling.

As a third possible explanation cholinergic or ghrelinergic stimulation might activate the inhibitory system, which then limits excitatory activity and impedes excessively synchronized firing. In general, ACh has an excitatory effect on excitatory cortical neurons and enhances the response of these neurons to other excitatory inputs. The excitatory effect as

well as the subsequent relaxation, is however much slower than that produced by glutamate or other excitatory amino acids, with a time constant of ~30 s. In a small percentage of neurons, Ach has been reported to be inhibitory. However, this is (almost) always caused by cholinergic excitation of inhibitory interneurons. Low threshold spiking interneurons are rapidly excited via activation of nicotinic receptors, whereas fast spiking inhibitory neurons were inhibited via muscarinic activation [41]. Thus, the predominant effect of cholinergic input would depend on the constitution of inhibitory neuronal types in the culture. If low threshold spiking neurons were to dominate, a rapid inhibition may be expected upon CCh application, which might initially outweigh the slow excitation. However, we observed increased network activity immediately after CCh application. Moreover, the reduced excitability lasted throughout the period of cholinergic activation. Therefore, it seems improbable that induced inhibition caused the reduced excitability. This conclusion is further supported by the finding that 10 day old cultures also showed more dispersed firing during activation. In 10 day old cultures, the inhibitory system is still in a very premature state of development.

Currently, hyper excitability is usually treated at the cellular level with medication that aims to reduce excitation or to enhance inhibition. Meanwhile, network activation, rather than inhibition, has hardly been explored to treat hyper excitability. Our findings support the hypothesis that hyper excitability may also result from insufficient network activation, and consequently may be treated by (moderate) network activation. In this case, traditional antiepileptic drugs targeted at reduction of activity, merely treat the symptoms and may in fact even deteriorate the hyper excitable network state. Stimulation techniques such as deep brain stimulation and vagal nerve stimulation have been shown to provide possible solutions to patients with refractory epilepsy [42, 43]. The mechanism of action behind these techniques remains largely unclear, but may involve moderate activation as used in this study.

In conclusion, we theoretically derived a parameter (SPRs) that excludes multiple input spike bias and therefore provides a cleaner measure of network excitability than conventional cross-correlation based measures such as CFPs. We validated that a change in the dynamic network state due to moderate pharmacological network activation affected the SPRs less than the CFPs. Whereas the differences between CFP values partially reflected multiple input spike bias, its persisting effect on SPRs indicates that mild activation decreases network excitability. This agrees with the reduced bursting observed after cholinergic or ghrelinergic activation and suggests that mild activation may offer yet unexplored opportunities to treat hyper excitability.

Acknowledgments

The authors wish to thank Dr Gerco Hassink and Karin Groot Jebbink from University of Twente, and Dr Marina Nanni and Claudia Chiabrera from NBT-IIT for the technical assistance in cell culture preparation, and Dr Yan Zhao for carefully proofreading the manuscript.

References

[1] Wagenaar D A, Madhavan R, Pine J and Potter S M 2005 Controlling bursting in cortical cultures with closed-loop multi-electrode stimulation *J. Neurosci.* **25** 680–8
[2] Daoudal G and Debanne D 2003 Long-term plasticity of intrinsic excitability: learning rules and mechanisms *Learn. Mem.* **10** 456–65
[3] Chiappalone M *et al* 2009 Opposite changes in glutamatergic and gabaergic transmission underlie the diffuse hyperexcitability of Synapsin I-deficient cortical networks *Cereb. Cortex* **19** 1422–39
[4] Patry G, Lyagoubi S and Tassinari C A 1971 Subclinical 'electrical status epilepticus' induced by sleep in children: a clinical and electroencephalographic study of six cases *Arch Neurol.* **24** 242–52
[5] Gratrix A P and Enright S M 2005 Epilepsy in anaesthesia and intensive care *Contin. Educ. Anaesth. Crit. Care Pain* **5** 118–21
[6] Boido D *et al* 2010 Cortico-hippocampal hyperexcitability in synapsin I/II/III knockout mice: age dependency and response to the antiepileptic drug levetiracetam *Neurosci.* **171** 268–83
[7] Dyhrfjeld-Johnsen J, Berdichevsky Y, Swiercz W, Sabolek H and Staley K J 2010 Interictal spikes precede ictal discharges in an organotypic hippocampal slice culture model of epileptogenesis *J. Clin. Neurophysiol.* **27** 418–24
[8] Harreby K R, Sevcencu C and Struijk J J 2011 The effect of spinal cord stimulation on seizure susceptibility in rats *Neuromodulation* **14** 111–6
[9] Stegenga J, le Feber J, Marani E and Rutten W 2010 Phase dependent effects of stimuli locked to oscillatory activity in cultured cortical networks *Biophys. J.* **98** 2452–8
[10] Corner M 2008 Spontaneous neuronal burst deischarges as dependent and independent variables in the maturation of cerebral cortex tissue cultured *in vivo*: a review of activity-dependent studies in live 'model' systems for the development of intrinsically generated bioelectric slow-wave sleep patterns *Brain Res. Rev.* **59** 221–44
[11] Chiappalone M, Corner M and le Feber J 2010 Persistent effects of cholinergic activation in developing cerebral cortex cultures: a model for the role of sleep activity patterns in early development? *7th Int. Meeting Substrate-Integrated Micro Electrode Arrays* (*Reutlingen, Germany*) (*BioPro*) ed A Stett pp 64–5
[12] Frega M *et al* 2012 Cortical cultures coupled to micro-electrode arrays: a novel approach to perform *in vitro* excitotoxicity testing *Neurotoxicol. Teratol.* **34** 116–27
[13] Steriade M and Amzica F 1999 Intracellular study of ecxcitability in the seizure-prone neocortex *in vivo* *J. Neurophysiol.* **82** 3108–22
[14] Eytan D and Marom S 2006 Dynamics and effective topology underlying synchronization in networks of cortical neurons *J. Neurosci.* **26** 8465–76
[15] Turrigiano G G, Leslie K R, Desai N S, Rutherford L C and Nelson S B 1998 Activity-dependent scaling of quantal amplitude in neocortical neurons *Nature* **391** 892–6
[16] Turrigiano G 2008 The self-tuning neuron: synaptic scaling of excitatory synapses *Cell* **135** 422–35
[17] Kilman V, van Rossum M and Turrigiano G 2002 Activity deprivation reduces miniature IPSC amplitude by decreasing the number of postsynaptic GABAa receptors clusterd at neocortical synapses *J. Neurosci.* **22** 1328–37

[18] van Pelt J, Wolters P S, Corner M A, Rutten W L C and Ramakers G J 2004 Long-term characterization of firing dynamics of spontaneous bursts in cultured neural networks *IEEE Trans. Biomed. Eng.* **51** 2051–62
[19] Romijn H J, van Huizen F and Wolters P S 1984 Towards an improved serum-free, chemically defined medium for long-term culturing of cerebral cortex tissue *Neurosci. Biobehav. Rev.* **8** 301–34
[20] Stegenga J, le Feber J, Marani E and Rutten W L C 2008 Analysis of cultured neuronal networks using intra-burst firing characteristics *IEEE Trans. Biomed. Eng.* **55** 1382–90
[21] Bologna L L *et al* 2010 Investigating neuronal activity by SPYCODE multi-channel data analyzer *Neural Netw.* **23** 685–97
[22] Chiappalone M, Bove M, Vato A, Tedesco M and Martinoia S 2006 Dissociated cortical networks show spontaneously correlated activity patterns during *in vitro* development *Brain Res.* **1093** 41–53
[23] le Feber J, Rutten W L C, Stegenga J, Wolters P S, Ramakers G J and Van Pelt J 2007 Conditional firing probabilities in cultured neuronal networks: a stable underlying structure in widely varying spontaneous activity patterns *J. Neural Eng.* **4** 54–67
[24] le Feber J, Van Pelt J and Rutten W 2009 Latency related development of functional connections in cultured cortical networks *Biophys. J.* **96** 3443–50
[25] Stoyanova I I, Wiertz R W F and Rutten W L C 2009 Time-dependent changes in ghrelin-immunoreactivity in dissociated neuronal cultures of the newborn rat neocortex *Regul. Peptides.* **158** 86–90
[26] Berardelli A, Rona S, Inghilleri M and Manfredi M 1998 Cortical inhibition in Parkinson's disease. A study with paired magnetic stimulation *Brain* **119** 71–7
[27] Eisenberg E, Chistyakov A V, Yudashkin M, Kaplan B, Hafner H and Feinsod M 2005 Evidence for cortical hyperexcitability of the affected limb representation area in CRPS: a psychophysical and transcranial magnetic stimulation study *Pain* **113** 99–105
[28] Langguth B, Eichhammer P, Marienhagen J, Kleinjung T, Sand P and Hajak G 2005 Low frequency repetitive transcranial magnetic stimulation (rTMS) in brain hyperexcitability disorders like tinnitus and auditory hallucinations *Plasticity and Signal Representation in the Auditory System* ed J Syka and M M Merzenich (New York: Springer) pp 329–34
[29] Bakker A *et al* 2012 Reduction of hippocampal hyperactivity improves cognition in amnestic mild cognitive impairment *Neuron.* **74** 467–74
[30] Chiappalone M, Massobrio P and Martinoia S 2008 Network plasticity in cortical ensembles *Eur. J. Neurosci.* **28** 221–37
[31] Shahaf G and Marom S 2001 Learning in networks of cortical neurons *J. Neurosci.* **21** 8782–8
[32] Chiappalone M, Vato A, Berdondini L, Koudelka-Hep M and Martinoia S 2007 Network dynamics and synchronous activity in cultured cortical neurons *Int. J. Neural. Syst.* **17** 87–103
[33] Kimura F, Fukuda M and Tsumoto T 1999 Acetylcholine suppresses the spread of excitation in the visual cortex revealed by optical recording: possible differential effect depending on the source of input *Eur. J. Neurosci.* **11** 3597–609
[34] Richardson R T (ed) 1991 *Current Status of the Basal Forebrain Cholinergic System: A Preview and Commentary* (Boston, MA: Birkhauser)
[35] Tateno T, Jimbo Y and Robinson H P 2005 Spatio-temporal cholinergic modulation in cultured networks of rat cortical neurons: evoked activity *Neuroscience* **134** 439–48
[36] Klink R and Alonso A 1997 Muscarinic modulation of the oscillatory and repetitive firing properties of entorhinal cortex layer II neurons *J. Neurophysiol.* **77** 1828–997
[37] Leondopulos S S, Boehler M, Wheeler B C and Brewer G J 2012 Chronic stimulation of cultured neuronal networks boosts low frequency oscillatory activity at theta and gamma with spikes phase-locked to gamma frequencies *J. Neural Eng.* **9** 026015
[38] Gil Z, Connors B W and Amitai Y 1997 Differential regulation of neocortical synapses by neuromodulators and activity *Neuron* **19** 679–86
[39] Bazhenov M, Timofeev I, Steriade M and Sejnowski T J 2002 Model of thalamocortical slow-wave sleep oscillations and transitions to activated states *J. Neurosci.* **22** 8691–704
[40] Markram H, Wang Y and Tsodyks M 1998 Differential signaling via the same axon of neocortical pyramidal neurons *Proc. Natl Acad. Sci. USA* **95** 5323–8
[41] Rasmusson D D 2000 The role of acetylcholine in cortical synaptic plasticity *Behav. Brain Res.* **115** 205–18
[42] Jones N 2010 Epilepsy: DBS reduces seizure frequency in refractory epilepsy *Nat. Rev. Neurol.* **6** 238
[43] Fisher R *et al* 2010 Electrical stimulation of the anterior nucleus of thalamus for treatment of refractory epilepsy *Epilepsia* **51** 899–908